Optimum finned space radiators

S. Sunil Kumar, Venketesh Nayak, and S. P. Venkateshan
Indian Institute of Technology, Madras, India

The present study considers a space radiator with uniform area fins standing vertically on a nonisothermal parent surface to enhance heat transfer. The numerical study shows that the finned radiator exhibits an optimum number of fins for which the heat lost from the finned radiator is a maximum, for given values of N_{R-C}, N_{F-C}, ε, and r_{OPT}. The numerical data has been used to derive correlations, respectively, between the optimum heat loss ratio and the optimum fin number with the other influencing parameters. These formulas are useful to the designer for a quick calculation of the performance of the optimum configuration.

Keywords: radiation conduction parameter; optimum fin number; heat loss ratio; irradiation

Introduction

In the design of spacecraft, one important problem that needs great attention is the dissipation of waste heat generated from power plants, from operation of equipment, and from other heat-generating units. Since radiation is the only mode of heat transport in space, a heat exchanger with extended surface fins offers the best means of increasing heat rejection from the system. Most of the work in the area of radiating fins with mutual interaction was developed between 1959 and 1963. Different radiator configurations were taken up by these researchers, e.g., the annular finned radiator and parallel pipes joined by webs acting as fins. Mackay (1963) and Karleker and Chao (1963) considered trapezoidal fins in great detail, of which the rectangular profile is a particular case. Mackay developed a numerical computation technique for designing space radiators with the assumption of a constant base temperature neglecting mutual irradiation. Sparrow et al. (1961) and Karleker and Chao (1963), although considering the mutual interaction between the fins, neglected the base interaction for a radiator with longitudinal fins on a cylindrical base. Base–fin interaction has been considered in some detail by Sparrow and Eckert (1962b). They drew attention to the fact that mutual base–fin interaction reduces total heat loss from the system significantly. A very penetrating and detailed analysis with respect to optimizing radiator mass has been provided by Karleker and Chao (1963).

Schnurr et al. (1974) considered circular fins of trapezoidal profile, and in 1976 they again considered circular fins of rectangular profiles, in both cases taking into account the base–fin interaction and mutual irradiation between fins. Tanaka et al. (1987) considered cases of nonisothermal surfaces but with convection. Unfortunately, all the studies carried out until now assume a constant base temperature that is valid for a condenser or an evaporator, thus conveniently avoiding a great deal of numerical difficulty but entertaining a large amount of tolerance in the optimized design. It is here the relevance of the present study comes in to picture.

Address reprint requests to Professor Venkateshan at the Heat Transfer and Thermal Power Laboratory, Department of Mechanical Engineering, Indian Institute of Technology, Madras 600036, India.

Received 6 December 1991; accepted 15 June 1992

In the present work, consideration is given to a radiator with rectangular fins that stand vertically, adjacent to each other, on a common nonisothermal parent surface that forms a side of a duct carrying hot fluid. The temperature of the fluid flow varies continuously along the duct, thus giving rise to a continuous change of the temperatures at the base of the fins. This geometry involves interaction between a fin with a base of continuously varying temperature, neighboring fins, and the ambient. The entire heat exchanger has to be treated as one system because of the conjugate nature of the problem. Temperatures and radiosities are to be obtained for all the surfaces making up the radiator. When radiation is combined with convection/conduction, the presence of both differential and integral terms having different powers leads to a set of nonlinear integrodifferential equations. The solution of the problem is complicated and time consuming. The massive expenditure and the high risks involved in the design of a space radiator, which is an integral part of space systems, make such comprehensive methods of analysis a necessity. A new term, *heat loss ratio*—the ratio of the heat lost by the finned radiator to the heat lost by the unfinned radiator, (q_{fr}/q_{ufr})—has been introduced, and its dependence on the radiation–conduction parameter, the increase in weight due to the addition of fins, and the number of fins, etc., have been studied. The existence of an optimum fin number for maximizing the heat loss ratio has also been established. Finally, a correlation has been given that quickly determines the maximum heat loss ratio as a function of various influencing parameters.

Some background to the present study

The first and most important issue is the relevance of the optimization that has been undertaken in the paper. It is commonly felt that optimum performance would be obtained for a black surface without fins. This question is addressed below by taking a specific example of a radiator with a single fin.

Example

Figure 1a shows a surface at temperature T_w and emissivity ε that is losing heat by radiation to a background effectively at

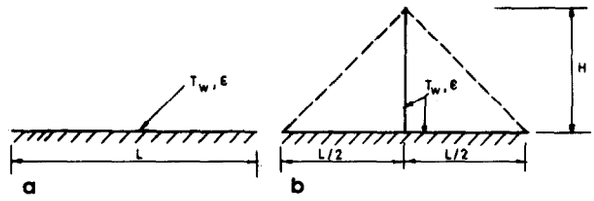

Figure 1 (a) Isothermal parent surface
Figure 1 (b) Parent surface with one fin added, all surfaces being isothermal

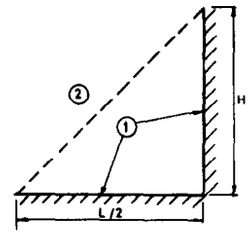

Figure 2 The two zones for analyzing the example problem

0 K. Figure 1b shows the configuration obtained by adding a surface of length H and surface emissivity ϵ to it at the middle and making a right angle with the parent surface. For simplicity, it is assumed that this surface is of infinite thermal conductivity and is of very small thickness. All the surfaces in configuration 1b are thus at T_w.

Configuration 1a loses an amount of heat per unit time and unit length in a direction perpendicular to the plane of the figure, given by

$$Q_{1a} = \varepsilon \cdot \sigma \cdot T_w^4 \cdot L \tag{1}$$

In the case of configuration 1b, we effectively have two enclosures formed as indicated by the dashed outlines and the basic surfaces. If we assume radiosities of the surfaces to be uniform (for simplicity), a simple enclosure analysis is possible. Figure 2 shows one such enclosure. Two zones are identified as indicated thereon. Zone 1 consists of the entire physical surface and zone 2 the opening of the triangular cavity. The requisite view factors are obtained by view-factor algebra. We have, from purely geometric arguments,

$$F_{21} = 1, \qquad F_{12} = \frac{(1 + (2H/L)^2)^{1/2}}{(1 + 2H/L)}, \qquad F_{11} = (1 - F_{12}) \tag{2}$$

The radiosity of opening $J_2 = 0$. The radiosity J_1 of the physical surface is given by

$$J_1 = \varepsilon \cdot \sigma \cdot T_w^4 + (1 - \varepsilon) \cdot F_{11} \cdot J_1$$

or, rearranging,

$$J_1 = \frac{\varepsilon \cdot \sigma \cdot T_w^4}{[1 - (1 - \varepsilon) \cdot F_{11}]} \tag{3}$$

The heat flux on the opening (zone 2) is given by

$$q_2 = (J_2 - F_{21} \cdot J_1) = -\varepsilon \cdot \sigma \cdot T_w^4 / [1 - (1 - \varepsilon) \cdot F_{11}] \tag{4}$$

Notation

Cp	Specific heat of the fluid, J/kg·K
dF	Diffuse view factor area product per unit width, m^2/m
F_{ij}	Diffuse view factor between zones i and j
g	Irradiation, W/m^2
H	Fin height, m
k	Thermal conductivity of the fin material, W/m·K
L	Length of the radiator, m
m	Mass flow of fluid, kg/m·s
n	Number of fins
n_1	Number of nodes along the fin
n_2	Number of nodes along the base
N_{R-C}	Black-body fin radiation conduction interaction parameter, nondimensional $= (\sigma T_{in}^3 H)/k$
N_i	Radiation conduction interaction parameter for fin i, nondimensional $= (\varepsilon \cdot \sigma \cdot T_{bi}^3 H^2)/(k \cdot 2t_x)$
N_{F-C}	Convection conduction interaction parameter, nondimensional $= (m \cdot Cp)/k$
N_{R-F}	Radiation convection interaction parameter, nondimensional $= (\varepsilon \cdot \sigma \cdot T_{in}^3 \cdot L)/(m \cdot Cp)$
N_{R-cl}	Radiation conduction interaction parameter for the heat exchanger, nondimensional, $(\sigma \cdot T_{in}^3 \cdot L/k)$
q	Heat loss from the radiator per unit width, W/m
r_{OPT}	Scaled optimum fin number parameter, nondimensional, $(n_{OPT} \cdot H)/L$
S	Spacing between the fins, m
S'	Length of the hypotenuse shown in Figure 4, m
$2t_x$	Fin thickness, m
T	Fin temperature, K
T_b	Base temperature, K
T_{in}	Fluid temperature at inlet, K
T_w	Temperature of all the surfaces in Figures 1a and 1b, K
x	Coordinate variable along the base, m
y	Coordinate variable along the fin, m

Greek symbols

β	Nondimensional heat loss from the unfinned radiator, $q_{ufr} \cdot /(\varepsilon \cdot \sigma \cdot T_{in}^4 \cdot L)$
ε	Emissivity of all exposed radiating surfaces
σ	Stefan–Boltzman constant, 5.67×10^{-8} $W/m^2 \cdot K^4$
θ	Nondimensional temperature, T/T_{bi}
ξ	Nondimensional coordinate along the fin, y/H
ϕ	Heat loss ratio $= q_{fr}/q_{ufr}$, nondimensional

Subscripts

b	Base
fr	Finned radiator
i	Fin number
j	Base between ith fin and $i + 1$th fin
L	Left surface of the fin
R	Right surface of the fin
Δx	Area element on the base
Δy	Area element on the fin
OPT	Optimum value
max	Maximum value
ufr	Unfinned radiator
∞	Environmental condition

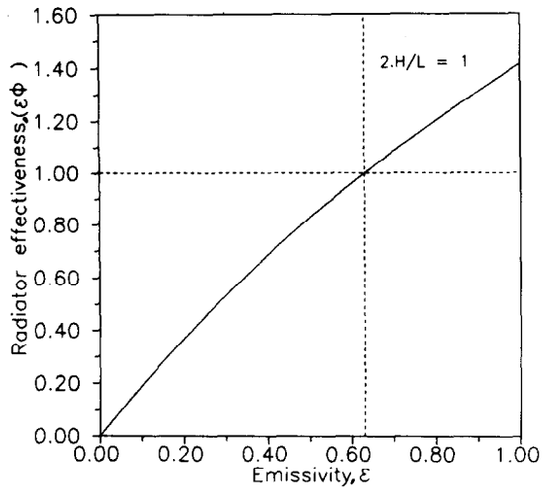

Figure 3 Emissivity vs. radiator effectiveness for a single isothermal fin system

Hence the heat loss from the two enclosures put together is

$$Q_2 = (2)\cdot(\text{opening area})\cdot(-q_2)$$

$$= \frac{(2)\cdot(H^2 + L^2/4)^{1/2}\cdot\varepsilon\cdot\sigma\cdot T_w^4}{[1-(1-\varepsilon)\cdot F_{11}]} \quad (5)$$

$$= (\varepsilon\cdot\sigma\cdot T_w^4\cdot L)\cdot\frac{[1+(2H/L)^2]^{1/2}}{1-(1-\varepsilon)\cdot\left\{1-\dfrac{[1+(2H/L)^2]^{1/2}}{(1+2H/L)}\right\}} \quad \text{(using Equation 2)} \quad (6)$$

We may define the heat loss ratio (ϕ) as

$$\phi = \frac{\text{Heat loss with fin}}{\text{Heat loss without fin}}$$

$$\phi = \frac{[1+(2H/L)^2]^{1/2}}{1-(1-\varepsilon)\cdot\left\{1-\dfrac{[1+(2H/L)^2]^{1/2}}{(1+2H/L)}\right\}} \quad (7)$$

It is seen that the heat loss ratio is invariably greater than or equal to unity. Specifically, for $\varepsilon = 1$, ϕ tends to $[1+(2H/L)^2]^{1/2}$ which is a consequence of the geometric increase in the effective area of the radiator.

It is to be noted that, in real life, the finite conductivity of the fins and the consequent temperature variation along it will reduce ϕ to a lower value. Equation 7 represents the upper limit to the advantage that is gained by the use of the fin.

We may also define a radiator effectiveness based on the parent surface at T_w and $\varepsilon = 1$. This is simply given by $(\varepsilon\cdot\phi)$. A plot of the radiator effectiveness as a function of ε is shown in Figure 3 for $2H/L = 1$ and infinite thermal conductivity. It is seen from this figure that the radiator effectiveness has an upper bound of $[1+(2H/L)^2]^{1/2} = 1.414$ and that $\varepsilon = 0.63$ represents the break-even point when the radiator loses the same amount of heat as the parent black surface. For $\varepsilon > 0.63$, the finned radiator loses more heat than the parent black surface.

In the case of a finite-thermal-conductivity fin, the temperature reduces monotonically from T_w at the base (in contact with the parent surface). The radiation interaction tends to reduce the temperature variation, while the conduction along the fin sets up a temperature variation along it. The fin length determines the relative effects of these two processes. Whereas Equation 7 shows a monotonic increase of heat loss ratio with H, the radiation–conduction interaction will lead to a compromise that makes it increase initially with increasing H, achieve a maximum at a certain H, and then decrease with further increase in H. Hence one expects an optimum ϕ for the simple finned radiator with a constant base temperature.

Finned-radiator case

In the case of the finned radiator considered in our paper, there are some differences due to the variation of temperature along the radiator and also along the fins. The two end fins correspond to the case considered above, and each has an increased effective "opening area," as shown in Figure 4 by the hypotenuse of length S'. Hence they have the dual advantage of an area increase of "opening" to the surroundings and the cavity effect, which increases the effective emissivity of the "opening." However, because of the temperature variation alluded to above, the cavity effect is reduced from the value that would have occurred if the system was isothermal. The intermediate fins involve the cavity effect, which increases the apparent emissivity of the opening. This state of affairs is indicated in Figure 4.

Existence of an optimum

Existence of an optimum fin number is a consequence of the following:

(1) the effects discussed above including the increase of the opening area of end fins in the radiator;
(2) cavity effect improves with closer spacing, leading to an enhanced effective emissivity; and
(3) temperature variation along the fin is affected by the spacing and fin height H to a significant extent.

In view of these facts, one would expect an optimum in the heat loss ratio. Also note that the parent radiator without fin would lose *less heat than an isothermal parent surface.* This is given by the quantity β later on in the paper.

The main point here is that the radiator without fin and $\varepsilon = 1$ does no lose the maximum heat, as is commonly felt.

Statement of the problem

The radiator under consideration is a rectangular duct losing heat from one side only, on which stand vertically rectangular profiled fins. The base lengths left of the first and right of the last fins are selected such that they are equal to half the spacing between any two intermediate fins (see Figure 5). All the surfaces are diffuse and have a uniform emissivity of ε. In general, heat transfer characteristics of a radiator are very complex. In condensers, the fluid temperature is uniform and constant from entrance to exit. But in radiators, this is not so.

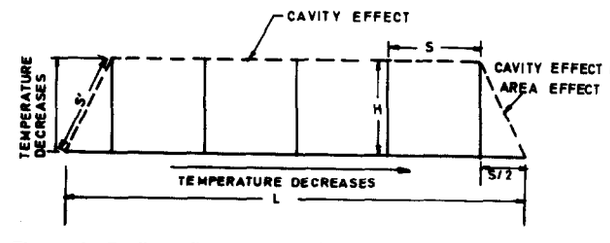

Figure 4 Radiator fin ensemble showing the nature of heat transfer enhancement for the middle and end fins

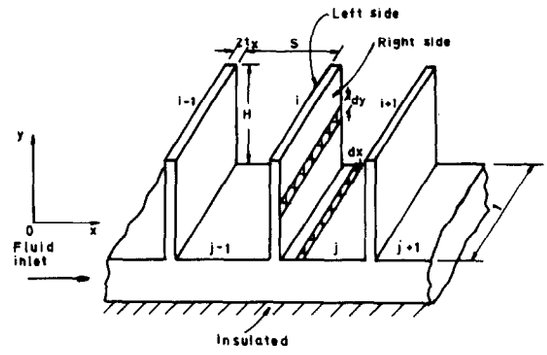

Figure 5 Radiator configuration considered in the present study. The geometry is defined and the elements used in making the energy balance are shown

The temperature variation of the base is, however, generally neglected in solving such problems, for simplicity. The inclusion of the variation of temperature complicates the calculation in two ways: (1) the symmetry assumption used otherwise is ruled out, and all the fins in the radiator will have to be treated individually; and (2) the temperature variation along each fin surface of the assembly will have to be evaluated separately. Hence, for each fin in the space radiator, we have two equations for the incident radiant flux for irradiation, one for the left and the other for the right surface. The energy equation on the fluid side also has to be included, since the problem is of conjugate nature. Essentially the problem is one in which the base temperature, T_b, is varying along the radiator.

Assumptions

(1) Heat loss from the surface is only by radiation.
(2) Uniform conditions exist in the environment, which is characterized by a temperature of T_∞ K.
(3) Material and surface properties of the radiator are constant and independent of temperature.
(4) The entire formulation of the problem is in the steady state.
(5) The local temperature of the fins is assumed to be constant across its thickness $2t_x$.
(6) Hence the fin heat transfer is treated basically as one-dimensional (1-D), and temperature variation is only in the y-direction.
(7) The radiator and the fin width are very large so that the end effects are negligible. At the tip, the heat conducted is equated to the heat lost by radiation.
(8) Resistance of the walls and the film on the liquid side of the heat exchanger are negligible, since the normally used fluids like the liquid metals have high heat transfer coefficients. Fluid flow is fully developed, and local fluid bulk temperature is assumed to be equal to the local base temperature.

Formulation

For the analysis of each fin, consider two enclosures, the left one comprising the left surface of the fin being considered, the right surface of the adjacent fin, the intermediate base, and the ambient, which is considered as a black body at an equivalent temperature of T_∞ K (Figure 6). Similarly, a right enclosure is drawn up. The governing equation for heat transfer in each fin will have two integral equations with slight modification for the first and last fins. The energy equation for the ith radiating–conducting fin is given by the following differential equation in the nondimenionalized form

$$d^2\theta_i/d\xi^2 = N_i \cdot \left[\theta_i^4 - \frac{1}{2\cdot\sigma\cdot T_{bi}^4}\{g_{i,L} + g_{i,R}\}\right] \tag{8}$$

with boundary conditions

(i) $d\theta_i/d\xi = -(\varepsilon\cdot\sigma\cdot(\theta_i^4 - \theta_{i\infty}^4)T_{bi}^3\cdot H/k)$ at $\xi = 1$

(ii) $\theta_i = 1$ at $\xi = 0$ (9)

where $\theta_{i\infty} = T_\infty/T_{bi}$ and $1 \leqslant i \leqslant n$. N_i is the familiar fin radiation–conduction interaction parameter.

Taking the energy balance on the fluid side, we have

$$T_{bi}(x) = T_{in} - q_i/m\cdot C_p \quad \text{for } 1 \leqslant i \leqslant n \tag{10}$$

Here the base temperature is assumed to be the fluid temperature at that location because of the high convective heat transfer rates involved on the fluid side, and q_i is taken as the heat lost up until the ith fin plus the heat lost by the left surface of the fin. The two integrals for irradiation, one for the left surface and the other for the right surface, are evaluated using Gebhart's method (Seigel and Howell 1972).

The equation for the irradiation on right surface of the fin is given by

$$\begin{aligned}\Delta y\cdot g_{i,R}(y) = {} & \varepsilon\cdot\sigma\cdot\int_0^S T_{bi}^4(x)\cdot dF_{\Delta x_j-\Delta y_i} \\ & + \int_0^S\int_0^H\left[(1-\varepsilon)\cdot\varepsilon\cdot\left\{\sigma\cdot T_i^4(y)\cdot\frac{dF_{\Delta y_i-\Delta x_j}}{\Delta x}\right.\right. \\ & \left.\left. + \sigma\cdot T_{i+1}^4(y)\cdot\frac{dF_{\Delta y_{i+1}-\Delta x_j}}{\Delta x}\right\}\right. \\ & \left. + (1-\varepsilon)^2\cdot\left\{g_{i,R}(y)\frac{dF_{\Delta y_i-\Delta x_j}}{\Delta x}\right.\right. \\ & \left.\left. + g_{i+1,L}(y)\frac{dF_{\Delta y_{i+1}-\Delta x_j}}{\Delta x}\right\}\right]dF_{\Delta x_j-\Delta y_i} \\ & + \int_0^H\left[\varepsilon\cdot\sigma\cdot T_{i+1}^4(y) + (1-\varepsilon)\cdot g_{i+1,L}(y)\right] \\ & \times dF_{\Delta y_{i+1}-\Delta y_i} + \sigma\cdot T_\infty^4\cdot F_{\infty-\Delta y_i} \\ & + (1-\varepsilon)\cdot\sigma\cdot\int_0^H T_\infty^4\cdot\frac{F_{\infty-\Delta x_j}}{\Delta x}\cdot dF_{\Delta x_j-\Delta y_i}\end{aligned} \tag{11}$$

For the left surface of the fin,

$$\begin{aligned}\Delta y\cdot g_{i,L}(y) = {} & \varepsilon\cdot\sigma\cdot\int_0^S T_{bj-1}^4(x)dF_{\Delta x_j-\Delta y_i} \\ & + \int_0^S\int_0^H\left[(1-\varepsilon)\cdot\varepsilon\cdot\left\{\sigma\cdot T_i^4(y)\cdot\frac{dF_{\Delta y_i-\Delta x_{j-1}}}{\Delta x}\right.\right. \\ & \left.\left. + \sigma\cdot T_{i-1}^4(y)\frac{dF_{\Delta y_{i-1}-\Delta x_{j-1}}}{\Delta x}\right\}\right. \\ & \left. + (1-\varepsilon)^2\cdot\left\{g_{i,L}(y)\cdot\frac{dF_{\Delta y_i-\Delta x_{j-1}}}{\Delta x}\right.\right. \\ & \left.\left. + g_{i-1,R}(y)\cdot\frac{dF_{\Delta y_{i-1}-\Delta x_{j-1}}}{\Delta x}\right\}\right]\cdot dF_{\Delta x_j-\Delta y_i} \\ & + \int_0^H\left[\varepsilon\cdot\sigma\cdot T_{i-1}^4(y) + (1-\varepsilon)\cdot g_{i-1,R}(y)\cdot\right] \\ & \times dF_{\Delta y_{i-1}-\Delta y_i} + \sigma\cdot T_\infty^4\cdot F_{\infty-\Delta y_i} \\ & + (1-\varepsilon)\cdot\sigma\cdot\int_0^H T_\infty^4\cdot\frac{F_{\infty-\Delta x_j}}{\Delta x}\cdot dF_{\Delta x_j-\Delta y_i}\end{aligned} \tag{12}$$

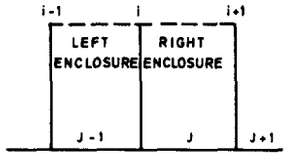

Figure 6 The two zones used in the analysis of an intermediate fin in the finned radiator

The irradiation on the base given by the following equation has been used to arrive at the above two equations.

$$\Delta x \cdot g_{b,j}(x) = \varepsilon \cdot \sigma \cdot \int_0^H T_{i+1}^4(y) \cdot dF_{y_{i+1}-\Delta x_j} + \varepsilon \cdot \sigma \cdot \int_0^H T_i^4(y) \cdot dF_{\Delta y_i-\Delta x_j} + (1-\varepsilon) \cdot \int_0^H g_{i,R}(y) \cdot dF_{\Delta y_i-\Delta x_j} + (1-\varepsilon_1) \cdot \int_0^H g_{i+1,L}(y) \cdot dF_{\Delta y_i-\Delta x_j} + \sigma \cdot T_\infty^4 \cdot F_{\infty-\Delta x_j} \quad (13)$$

Method of solution

An iterative procedure for nonlinear equations has been found to produce quick results for the required solution of the integrodifferential system of equations. A flow chart showing the calculation scheme is given in Figure 7. There are three different iterations involved here, two local iterations for the fins individually and another global iteration for the radiator as a whole. The global iteration is to achieve the convergence for the base temperature profile, which influences the fin temperatures indirectly and the irradiation on the fin surfaces directly, which in turn determines the base temperature profile. Moreover, there is a loss of symmetry due to the base temperature variation, making the calculation of radiation variables for one fin alone insufficient. Consider one fin, say the first one in Figure 3: it receives irradiation from the ambient on the left side and from the second fin on the right side whose radiosities are as yet unknown because they in turn depend on the radiosities of the first fin. Hence, initial values of the temperature profiles are calculated for all the fins, neglecting mutual interaction but including base temperature variation. This further explains the necessity for a global iteration. The first of the two local iterations consists of the solution of the governing differential equation for each fin, which is a boundary-value problem and is solved by a second-order RUNGE-KUTTA method that has a local truncation error of $O(h^3)$. The second iteration is for the convergence of the temperature and irradiation profiles of the fin. Here we start from the tip of the fin where the boundary condition is $d\theta_i/d\xi(n_1) = \varepsilon \cdot \sigma \cdot H \cdot (\theta_i^4 - \theta_{i\infty}^4) \cdot T_{bi}^3/k$. Assuming a temperature at the tip, the Runge–Kutta procedure proceeds up to the base backwards. The percentage error between the boundary condition at the base and the calculated value of $\theta_i(O)$ is then checked to see if the difference is within the desired limits. If this is not so, the procedure is repeated with a different value for $d\theta_i/d\xi(n_1)$. Iteration is continued until the desired covergence is encountered. The integral equation is solved by the Simpson formula, which is modified to incorporate the evaluation of double integrals. The intervals of the two numerical methods used here have been selected such that their respective truncation errors are the same. This was found to work satisfactorily without any instabilities for all calculations performed in the present study. In the iteration for the convergence for the irradiation values, the double integrals only need to be reevaluated in Equations 11 and 12 because

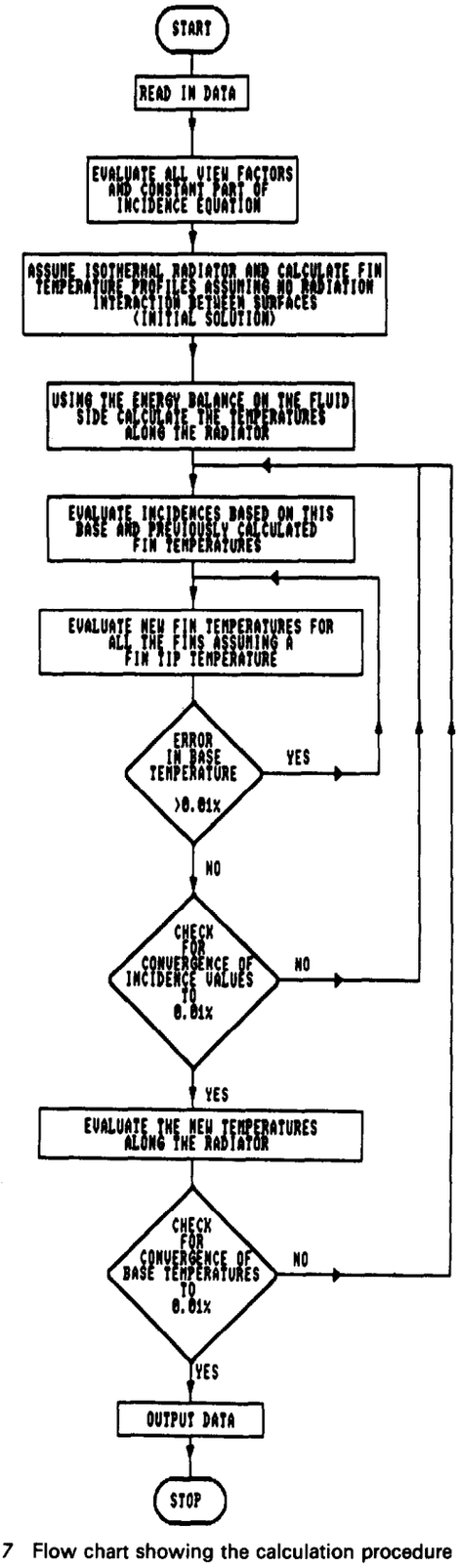

Figure 7 Flow chart showing the calculation procedure

Table 1 Ranges of variables used in the present numerical study

Quantity	Values used	Units
Fluid inlet temperature, T_{in}	350, 450, 750	K
Background temperature, T_∞	0	K
Thermal conductivity, k	54, 110, 257	W/m·K
Length of the radiator, L	0.5, 0.75, 1	m
Number of fins, n	6–30	—
Mass flow sp. heat product, mC_p	3, 7.5, 14	W/m·K
Emissivity, ε	0.5, 0.65, 0.75, 0.9	—
Fin height, H	0.06–0.185	m
Fin thickness, $2t_x$	0.0005, 0.00075 0.001, 0.0015	m

the rest of the terms, once evaluated, remain constant. Also to be noted is that for the double integrals the iteration proceeds first with respect to H and then with respect to S.

To get the temperature $T_i(y)$ from the differential equation (Equation 8), we have to know $g_{i,L}(y)$ and $g_{i,R}(y)$. For finding these values, a first aproximation is made for the irradiation, say, that part of the incident radiation that comes from the ambient and this value is inserted into Equation 8. Now Equation 8 is solved by the above-mentioned method to get the temperature profile. This temperature profile and the approximate irradiation values taken before are introduced into Equations 11 and 12 to get the new value of irradiation. This procedure is continued until the values of $T_i(y)$, $g_{i,L}(y)$, and $g_{i,R}(y)$ converge to within a specified tolerance. Thus the temperature and the irradiation values at all the nodes along the fins and the base are obtained. This procedure is repeated for every main iteration.

One feature of the present solution method is the use of the crossed-string method for calculation of view factors because the fins are assumed very long in the third direction. This method makes a rather tedious task relatively simple. However, with some extra computation one can, if interested, calculate for a finite length in the third direction also.

Results and discussions

The performance of the radiator has been analyzed, with emphasis on the fin spacing for different material properties and the geometry of the radiator. The base temperature variation produces a change in the radiation–conduction interaction parameter N_i for the fins along the radiator. A convergence study showed that 20 nodes were sufficient for both the fin and the base length in the interfin space for the convergence of the fin temperature and of the incidence profile within a tolerance limit of 0.01 percent. The program was also checked for fins without any interfin or fin base interaction, and the results agreed with previous calculations of Karleker et al. (1963).

The typical range of parameters taken into consideration in the present study is given in Table 1. The choice of the parameters is governed by the range of values for the thermophysical properties encountered in practice and is also guided by the fact that emissivity of the surface should be high for good heat transfer. Emissivity less than about 0.5 is seldom used, and hence we have explored the performance of the radiator for $\varepsilon \geq 0.5$ only. The radiator will face away from any strong background-radiation sources like planets or the sun and is characterized by a temperature very much lower than the radiator surface temperature—it may effectively be considered as 0 K. However, the calculation may be extended for $T_\infty \neq 0$ with little effort. The total number of calculations that have been made is around 500. Each calculation takes about 80 CPU seconds on the SIEMENS 7580E system. This set yields about 45 data points for obtaining the correlation for the maximum heat loss ratio that is presented later on.

Temperature profiles

Consider first the variation of base temperature along the radiator. The smooth profile in Figure 8 that is obtained by plotting the temperatures along only the base of the fins shows a linear variation, while the actual base temperature variation is far from linear and is shown by the staircaselike profile. It shows a linear variation in the space between the fins, while a steep drop is observed as we approach a fin and move away from it, in its immediate vicinity. As expected, the base temperature values increase with decreasing emissivity (Figure 9).

Turning attention to the fin temperature profiles, Figure 10 shows the temperature profiles along the fins. A consistent feature is that, although N_i decreases progressively with fin position (i.e., from fin 1 to fin 12 in Figure 10) because of the decrease in base temperature, the fin-temperature profile of the last fin (fin 12) has a steep downward trend compared to that of the middle fins (fins 2 to 11) but stays above that of the first fin (fin 1) because of its lower N_i value. This is because of the asymmetry in the irradiation on the first and last fins. Also noticeable is the very small variation in temperature profiles of the intermediate fins. The first and last fins thus group together, and the intermediate fins form another goup with respect to the variation of temperature profiles with N_i.

Heat loss ratio

Figures 11 and 12 show the variation of heat-loss ratio (ϕ) with the number of fins in the radiator. The general trend the graphs exhibit is that as more and more fins are added to the radiator, the heat loss ratio initially increases steeply and reaches a maximum and decreases gradually thereafter. The point of maximum ϕ is the point of optimum fin number, n_{OPT}, for that

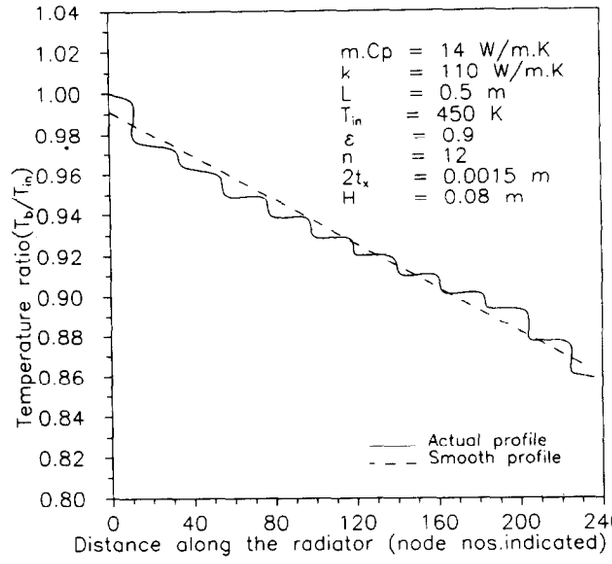

Figure 8 Actual and smooth temperature profile along the radiator for a typical case

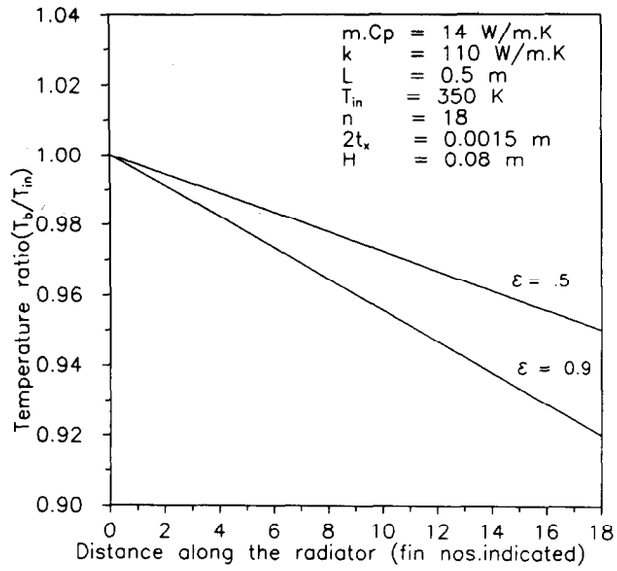

Figure 9 Variation of smoothed fin root temperature along the base for two different values of ε

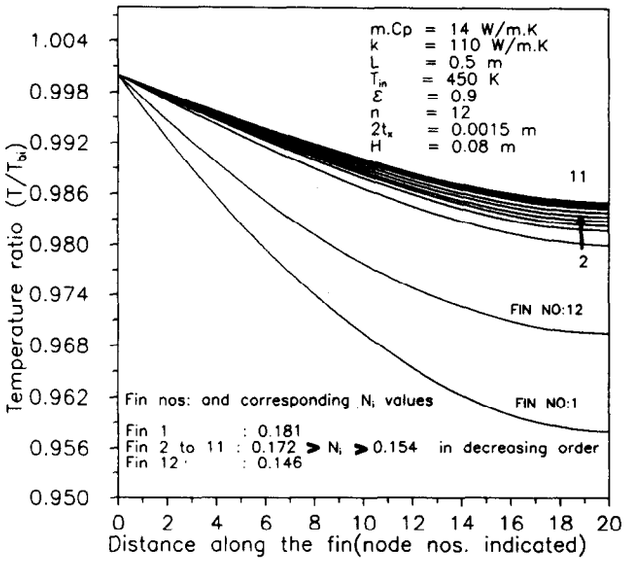

Figure 10 Temperature profile along the fin in a radiator consisting of 12 fins. Data set is identical to the typical case shown in Figure 8

particular radiator–fin geometry. The presence of an optimum fin number is ascribed to the fact that as the number of fins is increased, there is an increase in the apparent emissivity due to the cavity effect, and a simultaneous reduction of view factors of the cavities to space. The temperature variation along the fin is affected by these two opposing factors and strikes a balance at n_{OPT}. Calculations have shown that the heat lost from the first and last fins amounts to a major portion of the total heat lost from the radiator. It is to be stressed here that as the number of fins are varied, the base lengths to the left of the first fin and to the right of the last fin (given by S/2 in Figure 4), with relatively low irradiation and thus capable of losing a significant amount of heat, also vary and thus play a significant role in positioning ϕ_{max}.

It was noticed that for a given thermal conductivity ϕ_{max} increased with fin height. The increase in ϕ_{max} is nonlinear, showing a tendency to stabilize after a given fin height. In fact for the particular case of emissivity 0.9 and number of fins 8, the system was found to have a ϕ_{max} of 1.40 for a fin height of 18.5 cm. The ϕ_{max} decreases with further increase in fin height. The emissivity, on the other hand, plays an opposite role with respect to fin height regarding ϕ_{max}—i.e., with increasing emissivity there is a decrease in ϕ_{max}. This is as expected, since the mutual interaction reduces with increasing ε. However, ϕ_{max} increases with decreasing ε, indicating that the finning of the radiator is more effective at lower ε although it loses much less heat. Another point to be noted is that as the number of fins is increased indefinitely, the heat-loss ratio goes below one (such cases are not shown in the figures), which means that we were better off with the parent surface itself before the addition of fins. Figure 13 shows the variation of ϕ with respect to the radiation–conduction parameter. It is observed that a higher

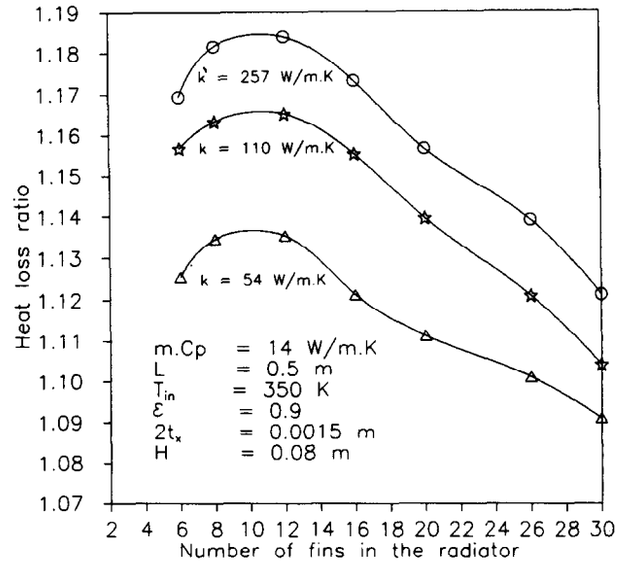

Figure 11 Heat loss ratio variation with number of fins for a radiator with different material thermal conductivities

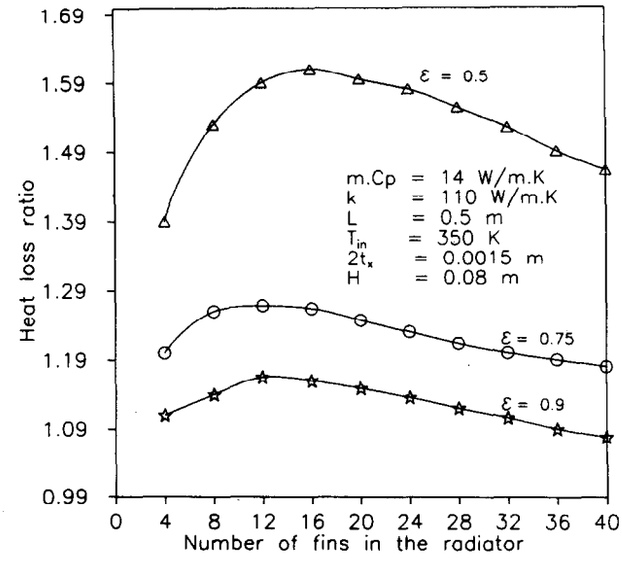

Figure 12 Heat loss ratio with number of fins for a radiator with different surface emissivities

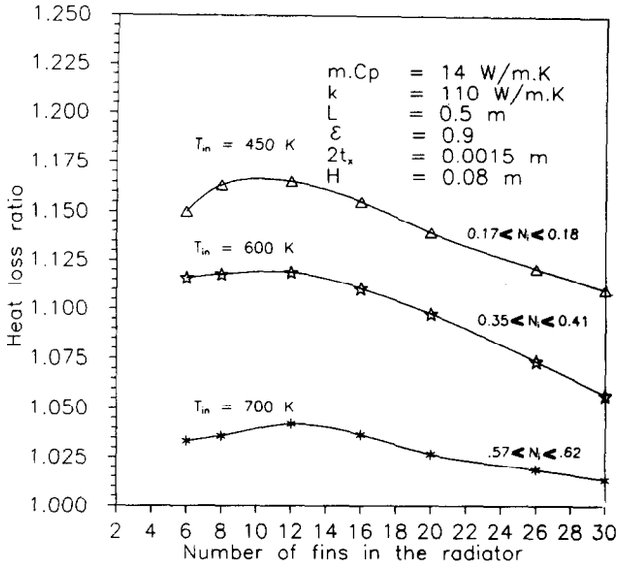

Figure 13 Variation of heat loss ratio with N_f obtained by varying fluid inlet temperature T_{in}

radiation–conduction parameter has a reduced ϕ_{max}. This is as expected, since this parameter is a measure of relative resistance to the heat transfer by conduction in the fin compared to the radiation from the surface.

Figure 14 compares the performance of the optimized radiator ensemble fabricated from three materials—brass, steel, and aluminum. The graph has been obtained by plotting the maximum ϕ for a given fin thickness and surface emissivity of 0.9 vs. the increase in weight due to the addition of fins. As expected, it clearly shows the relatively superior performance of aluminum over brass and steel. Also notice that steel shows a significant leveling off with increasing radiator weight partly due to the nonlinear increase in the n_{OPT} with fin height and partly due to its very high density. This enables the designer to fix the limits for the satisfactory working of the system for a particular material.

Correlation

It is well known that the radiative heat loss from a fin increases steeply with fin thickness. Starting from zero, it reaches a local maximum and then the variation of heat loss with respect to thickness is not appreciable over a range of thicknesses (Kern and Kraus 1972). All the calculations done here have been made in this range (note that this thickness range is necessary in practice in order to satisfy strength requirements) so the change in thickness shown in Table 1 has negligible effect on the positioning of ϕ_{max}.

Out of roughly 500 data sets obtained by performing the calculations for all the combinations of the range of variables indicated in Table 1, 45 data set corresponded with optimum ϕ. Though calculations have been made for lower values of thermal conductivity (57 W/m K), for the correlation we have restricted ourselves to cases of higher values of k, since the normally used material for space application is aluminum, which has a high thermal conductivity. Recognizing that ϕ_{max} should depend on the four parameters N_{R-C}, N_{F-C}, r_{OPT}, and ε, a correlation was obtained for ϕ_{max} as

$$\phi_{max} = 0.652\, N_{R-C}^{-0.0808} N_{F-C}^{0.0342} r_{OPT}^{0.155} \varepsilon^{-0.474} \qquad (14)$$

which fits the numerical data with a correlation coefficient of 0.997. The range of various parameters are

$$0.0003 < N_{R-C} < 0.02, \qquad 0.03 < N_{F-C} < 0.13,$$

$$0.78 < r_{OPT} < 4.07, \qquad 0.5 \leqslant \varepsilon \leqslant 0.9$$

The values of ϕ_{max} vary between 1.04 and 1.65 over the above range of the governing parameters.

A straightforward analysis yields a nondimensional heat loss for the unfinned radiator as

$$\beta = \frac{1}{N_{R-F}}\left[1 - \frac{1}{(1 + 3 \cdot N_{R-F})^{1/3}}\right] \qquad (15)$$

which is always less than unity. This is so since an unfinned radiator can lose less heat than $\varepsilon \cdot \sigma \cdot T_{in}^4 \cdot L$ because of the temperature variation along the radiator even in the absence of fins. The product of ϕ_{max} and β will in fact yield the actual nondimensional heat loss for the finned radiator in the optimum configuration. Thus from a design viewpoint, Equations 14 and 15 yield a simple method for calculating the performance of an optimum finned radiator once the thermophysical properties are fixed. The regression fit shows that the optimum heat loss ratio is strongly affected by both the fin number parameter r_{OPT} and the surface emissivity ε.

Another correlation has also been brought out to determine the optimum fin number parameter, r_{OPT}, as follows:

$$r_{OPT} = 6.3\, N_{F-C}^{0.05} \cdot (1 + \varepsilon^{-0.2}) \cdot (H/L)^{0.925} N_{R-Cl}^{0.0123} \qquad (16)$$

with an identical range of parameters as for Equation 14 and $0.038 < N_{R-Cl} < 0.14$. From Equation 16, n_{OPT} can be found by the relation $n_{OPT} = (r_{OPT} \cdot L/H)$ for the particular geometry. This value of n_{OPT} is inserted into Equation 14 to evaluate the corresponding ϕ_{max}.

The regression fit and the numerical data of the maximum heat loss ratio are in excellent agreement with a maximum error of ± 4 percent and are shown in Figure 15. There is some scatter however, for data obtained with higher emissivity values. This is explained by referring back to Figure 12, which shows that the variation of ϕ with the number of fins is rather mild and yields ϕ values over a range of fin numbers bracketing n_{OPT} close to ϕ_{max}, especially for $\varepsilon = 0.75$ and $\varepsilon = 0.9$. Also the value of n_{OPT} has to be a whole number, and

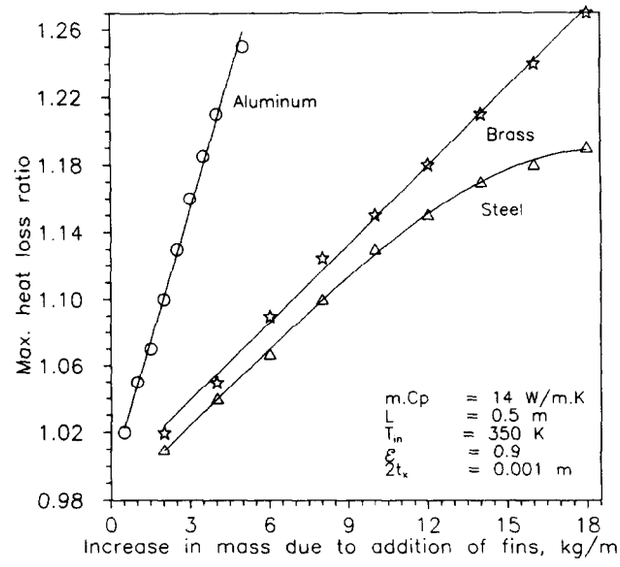

Figure 14 Variation of maximum heat loss ratio with increase in weight due to the addition of fins for three different materials

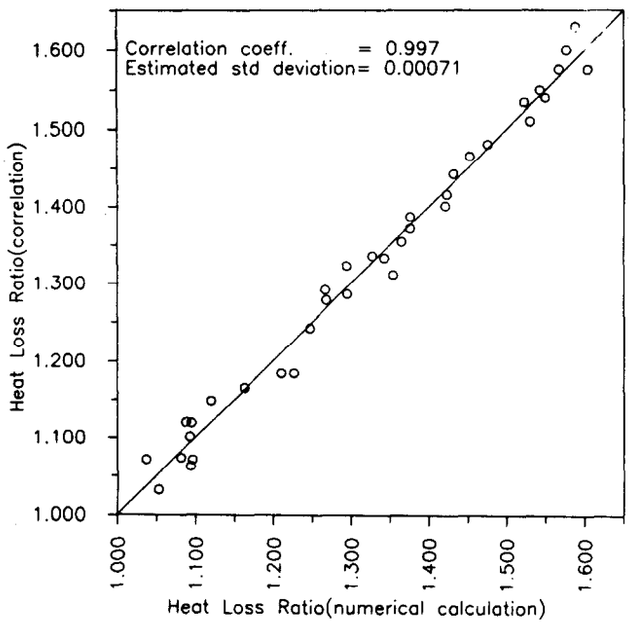

Figure 15 Comparison of correlated result with numerical data for ϕ_{max}

hence ϕ_{max} is not sharply defined. This translates to an uncertainty, which is apparent from Figure 15. In fact, while using Equation 16 to determine n_{OPT} for given values of other parameters, it may so happen that n_{OPT} is not a whole number. In that case the designer has to round off the value to the nearest whole number, with an attendant departure of ϕ_{max} from the value based on Equation 15. So in essence the designer may use the three relations 14, 15, and 16 to find the approximate value of ϕ_{max} of interest and if necessary can do the calculation using the formulation given to achieve greater accuracy.

In order to further highlight the efficacy of the proposed correlation, we compare in Table 2 the values of n_{OPT} and ϕ_{max} obtained from the computed data set and the correlation, respectively, for extreme values of parameters shown therein. The calculated values from the correlation and the numerical data are in very close agreement, and hence the correlation mirrors the variation of ϕ_{max}, and n_{OPT} with the various parameters very well. Note particularly that the variation with respect to ε in Equation 16 is not of the power-law type. Regression using a power-law type gave decidedly poorer fits. A detailed analysis of the data sets with different ε values finally yielded the factor $(1 + \varepsilon^{-0.2})$ in Equation 16. Thus we can use the proposed correlation with confidence for obtaining the weight-optimized design for the radiator, as will be done below.

Weight optimization of the radiator

The whole optimization procedure followed above is from thermal point of view, and is only a partial optimization since there is a weight increase as a penalty. A weight optimization is therefore called for, but it is highly involved, and the conventional methods do not work because of the increased number of degrees of freedom introduced by the nonisothermal base. Even if one were to do this, it is well known that the minimum-weight fin will be so thin as to be impossible to fabricate, and hence in actual practice it will be limited by the strength of the material to withstand the working conditions (see Mackay 1963). Consequently, the present procedure can be used effectively to find the optimum design by using the correlation given above. This can be carried out in two ways: (1) minimum weight for the dissipation of a desired quantity of heat, and (2) maximum heat loss for a particular weight addition.

For the first case, once the thermophysical properties are fixed, the value of r_{OPT} is found from Equation 14, fixing a small value for H. This value of r_{OPT} yields a value of n_{OPT} that is then rounded off to the nearest whole number. Now a minimum required thickness for sufficient strength is selected, and the weight of the fins are found. The procedure is repeated step by step for different heights, and the respective weights are found. This one set of calculations will result in a minimum weight that will give the optimum weight addition for the desired performance. This method is illustrated in Figure 16 for two different sets of conditions. For each set it can be seen that there exists a minimum weight configuration (indicated by points A and B in Figure 16) that gives optimum design. In fact, if the thickness of the fin is kept constant for increasing heights, one can observe a downward trend for the mass added (shown by dashed lines)—which is not practicable, since a longer fin should be thicker to withstand its own weight and the flight conditions. Therefore, in actual practice the thickness should be varied with height of the fin so as to satisfy the strength criteria. For example, of the two curves, one corresponds to a ϕ_{max} of 1.30. Here initially, a fin thickness of 0.5 mm is assumed for the first five heights (3, 4, 5, 6, and 7 cm) and is increased in steps of 0.05 mm thereafter.

In the second method, r_{OPT} is found by using Equation 16, and the corresponding n_{OPT} value is rounded off to a whole number as before. Calculations begin with a small value of H that is to be increased step by step. For each step, ϕ_{max} and the thickness of the fin are found by using Equation 14 and the known weight addition. In this procedure, one again chooses a combination that will give a comparatively high value for ϕ_{max}, with the thickness not less than that which will be unacceptable from the strength consideration. This configuration is taken as the optimum design for maximum ϕ. Figure 17 shows the variation of ϕ_{max} with addition of weight.

Table 2 Comparison of numerical data and calculation based on correlation for extreme values of some of the governing parameters

				Numerical data		From correlation	
ε	T_{in} K	H_m	L_m	n_{OPT}	ϕ_{max}	n_{OPT}*	ϕ_{max}
0.5	350	0.060	0.50	12	1.60	12	1.59
0.5	750	0.185	0.50	11	1.42	12	1.41
0.5	350	0.060	1.00	13	1.44	13	1.44
0.5	750	0.185	1.00	12	1.29	12	1.29
0.9	350	0.060	0.50	12	1.21	12	1.21
0.9	750	0.185	0.50	11	1.08	11	1.07
0.9	350	0.060	1.00	13	1.10	12	1.09

* These values are rounded off as suggested in the text

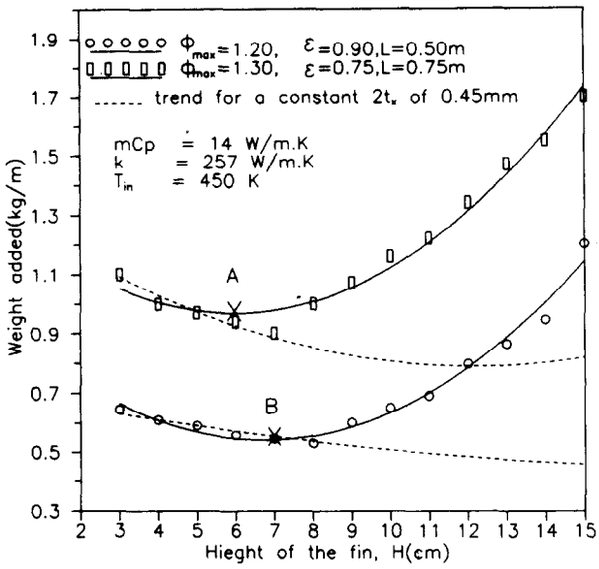

Figure 16 Minimum weight design for a given heat load using aluminum fins. The minimum weight points are represented by *X*

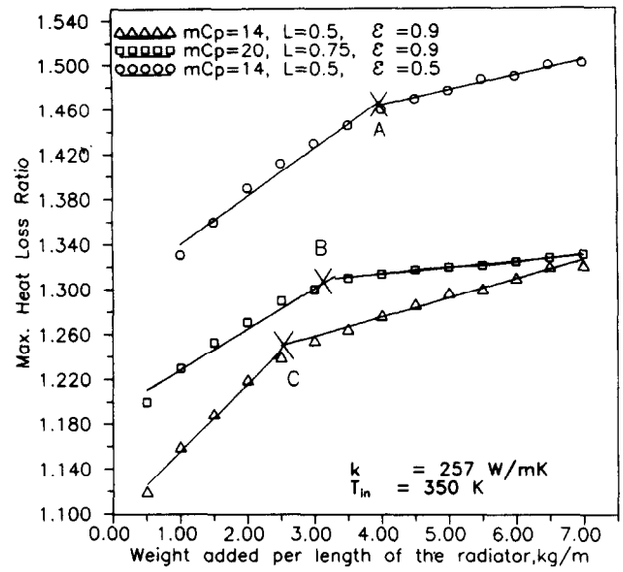

Figure 17 Distribution of ϕ_{max} with respect to weight addition for aluminum-finned radiator. The optimum configurations are shown by *X*

It can be observed that the increase of ϕ_{max} is very steep initially, but after a particular value of mass addition (indicated by *X*) is very nominal and is not worth adding. This point is referred to as the optimum configuration for a radiator system. However, a thicker fin is used in this case than in the examples considered in Figure 16, and this effectively increases the added weight for comparatively the same value of ϕ_{max}.

Conclusions

The above analysis for a finned radiator has shown the existence of an optimum number of fins for achieving a maximum heat loss ratio. The numerical data have been used to arrive at a useful correlation for determining ϕ_{max} in terms of the two interaction parameters N_{R-C} and N_{F-C}, a scaled fin number parameter r_{OPT}, and the surface emissivity ε. Further work is to be directed towards cases involving fins of nonuniform area. Also of interest would be tubular radiators with circumferential fins, which probably are more suitable for application where available space is limited. The weight-optimization study in these cases will be a challenging one. Work is ongoing in this area, and the results will be published elsewhere.

The analysis presented in this paper can be studied by taking into account the fluid-side heat transfer coefficient. The equality of the wall and fluid temperature is certainly a limiting situation valid for a very high heat transfer coefficient on the fluid side. As indicated in the paper, a liquid-metal situation will correspond to this. The temperature at entry also has been chosen in the range 350–900 K, in view of this. For situations other than these, the temperature of the wall and fluid are certainly different. These can be taken into account without much difficulty. It involves, however, an additional parameter given by $h/m \cdot C_p$ (h = fluid-side heat transfer coefficient). It is not difficult to assume an average fluid-side heat transfer coefficient and to do the calculations. In fact, such calculations have shown that the dependence of ϕ_{max} on heat transfer coefficient is not very appreciable. The results presented here may be used if the value of $h/m \cdot C_p$ is greater than 200.

References

Bartas, J. G. and Sellers, W. H. 1960. Radiation fin-effectiveness. *Trans. ASME J. Heat Transfer*, **82**, 73–75

Chen-Ya, Liu. 1960. On minimum weight rectangular radiating fins. *J. Aero Space Sci.*, **27**, 871–872

Hildebrand, F. B. 1974. *Introduction to Numerical Analysis*, second ed. McGraw-Hill, New York

Karleker, B. V. and Chao, B. T. 1963. Mass minimization of radiating trapezoidal fins with negligible base cylinder interaction. *Int. J. Heat Mass Transfer*, **6**, 33–48

Kern, D. Q. and Kraus, A. D. 1972. *Extended Surface Heat Transfer*. McGraw-Hill, New York

Mackay, D. B. 1963. *Design of Space Power Plants*, first ed. Prentice-Hall, Englewood Cliffs, NJ, 221–269

Nilson, E. N. and Curry, R. 1960. Minimum weight straight fin of triangular profile radiating to space. *J. Aero Space Sci.*, **27**, 146–147

Siegel, R. and Howell, J. R. 1972. *Thermal Radiation Heat Transfer*. McGraw-Hill Kogakusha Ltd., Tokyo

Sparrow, E. M., Eckert, E. R. G. and Irvine, T. F. 1961. The effectiveness of radiating fins with mutual irradiation. *J. Aero Space Sci.*, **28**, 763–778

Sparrow, E. M., Miller, E. B. and Jonsson, V. K. 1962a. Radiating effectiveness of annular finned space radiators. *J. Aero Space Sci.*, **29**, 1291–1299

Sparrow, E. M. and Eckert, E. R. G. 1962b. Radiant interaction between fin and base surfaces. *ASME J. Heat Transfer*, **84**, 12–18

Schnur, N. M. and Cothran, C. A. 1974. Radiation from an array of gray circular fins of trapezoidal profile. *AIAA J.*, **12**, 1476–1480

Schnurr, N. M. Shapiro, A. B. and Townsend, M. A. 1976. Optimization of radiating fin arrays with respect to weight. *J. Heat Transfer*, **98**, 643–648

Tanaka, S., Yoshida, T. and Kunitomo, T. 1987. Optimization of heat transfer for a vertical fin array on isothermal and non-isothermal plane surfaces with combined natural convection and radiation. *Heat Transfer Jpn. Res.*, **16**, 91–112

Wilkins Jr., J. E. 1960. Minimizing the mass of radiating fins. *J. Aero Space Sci.*, **27**, 145–146